Journal of Materials Science & Technology 39 (2020) 74–81

Contents lists available at ScienceDirect

Journal of Materials Science & Technology

journal homepage: www.jmst.org

Research Article

Cyclic shear deformation and fatigue of extruded Mg-Gd-Y magnesium alloy

Fenghua Wang [a,d], Miaolin Feng [b], Yanyao Jiang [c], Jie Dong [a,*], Zhenyan Zhang [a,d]

[a] National Engineering Research Center of Light Alloy Net Forming & State Key Laboratory of Metal Matrix Composites, Shanghai Jiao Tong University, Shanghai, 200240, China
[b] Department of Engineering Mechanics, Shanghai Jiao Tong University, Shanghai, 200240, China
[c] Department of Mechanical Engineering, University of Nevada, Reno, NV, 89557, USA
[d] Shanghai Light Alloy Net Forming National Engineering Research Center Co. Ltd, Shanghai, 201615, China

ARTICLE INFO

Article history:
Received 18 June 2019
Received in revised form 1 August 2019
Accepted 12 August 2019
Available online 26 September 2019

Keywords:
Mg-Gd-Y-Zr magnesium alloy
Cyclic torsion
Shear fatigue
Twinning

ABSTRACT

Deformation and fatigue of extruded Mg-8.0Gd-3.0Y-0.5Zr (GW83, wt%) magnesium (Mg) alloy were experimentally investigated under cyclic torsion using tubular specimen fabricated along the extrusion direction. The controlled shear strain amplitudes ranged from 0.606% to 4.157%. Twinning and detwinning of extension twins are observed to take place during cyclic torsion and the shear stress-shear strain hysteresis loops display a perfectly symmetric shape at all tested strain amplitudes. Marginal cyclic softening is observed when the shear strain amplitude is higher than 1.732%. The strain-life fatigue curve shows two kink points, corresponding to the shear strain amplitude of 1.040% and 1.732%, respectively. When the shear strain amplitude is higher than the upper kink point, early fatigue crack is found to initiate on the maximum shear plane. When the strain amplitude is lower than the lower kink point, fatigue cracking is parallel to the maximum tensile plane. At an identical equivalent strain amplitude, the fatigue life under pure shear is much higher than that under tension-compression. The fatigue life of extruded GW83 alloy is much higher than that of extruded AZ31B alloy at the same plastic strain energy density.

1. Introduction

Wrought magnesium (Mg) alloys have attracted attention as structural materials in the aerospace and automotive industries due to low density and high mechanical property [1,2]. Load bearing structural components are usually subjected to cyclic loading. The stress state influences the fatigue behavior. It is, therefore, necessary to characterize the fatigue behavior of wrought Mg alloys under different stress states.

Conventional wrought Mg alloys usually present a strong basal texture during plastic deformation [3,4]. Extensive studies have been conducted on monotonic and cyclic deformation of conventional wrought Mg alloys. Under monotonic loading, a conventional wrought Mg usually displays pronounced tension-compression asymmetry [5–7]. Extension twinning is activated when compression is applied along the extrusion direction (ED) or along the rolled direction. In cyclic tension and compression, the shape of the stress-strain hysteresis loop closely depends on the strain amplitudes [8]. The twinning and detwinning of extension twins occur alternately in extruded Mg alloys loaded along the extrusion direction at high strain amplitudes [9,10]. The directional nature of twinning activation results in the asymmetric shape of the stress-strain hysteresis loop under cyclic loading.

With addition of rare earth (RE) elements, wrought Mg-RE alloys have a weaker texture, higher mechanical property, and lower anisotropy [11,12] as compared with the conventional Mg alloys. The extruded Mg-Gd-Y-Zr alloys present a smooth stress-strain curve and display a yielding symmetry in monotonic tension and compression [13,14]. It shows near-symmetric stress-strain hysteresis loops at high strain amplitudes under the cyclic tension-compression due to insignificant extension twinning [13].

Free end torsion of a tubular specimen creates a pure shear stress state. Pure shear is an important stress state as compared with tension and compression [15,16]. Dislocation slip and mechanical twinning are important plastic deformation mechanisms during

* Corresponding author.
E-mail address: jiedong@sjtu.edu.cn (J. Dong).

https://doi.org/10.1016/j.jmst.2019.08.025
1005-0302/

free end torsion in Mg alloys. The volume fraction of extension twin is closely related to shear strain and independent on the loading direction. Swift effect, i.e., the second-order axial effect during free end torsion, is mainly resulted from extension twinning [17]. Effects of free end torsion on the microstructure evolution and mechanical properties of conventional wrought Mg alloys were investigated [18–20]. Pre-torsion deformation was employed to optimize texture, to improve mechanical properties and to reduce anisotropy. For instance, the tensile and compressive properties were improved via a simple pre-torsion for extruded AZ31 alloy [19,20]. Experiments under cyclic torsion of conventional wrought Mg alloys were conducted in recent years [21–24]. A symmetric shape of stress-strain hysteresis loop was observed at all shear strain amplitudes tested under cyclic torsion [23]. Although twinning and detwinning were involved in cyclic torsion at high strain amplitudes, the shear stress-shear strain hysteresis loops were still symmetrical [21]. However, there were only a few investigations on cyclic torsion and shear fatigue of the weak textured Mg alloy.

Mg-8.0Gd-3.0Y-0.5 Zr (GW83) alloy is a typical weak texture and high strength Mg-RE alloy as compared with conventional wrought Mg alloys. This paper studies the deformation and fatigue of an extruded GW83 alloy under cyclic torsion along the extrusion direction.

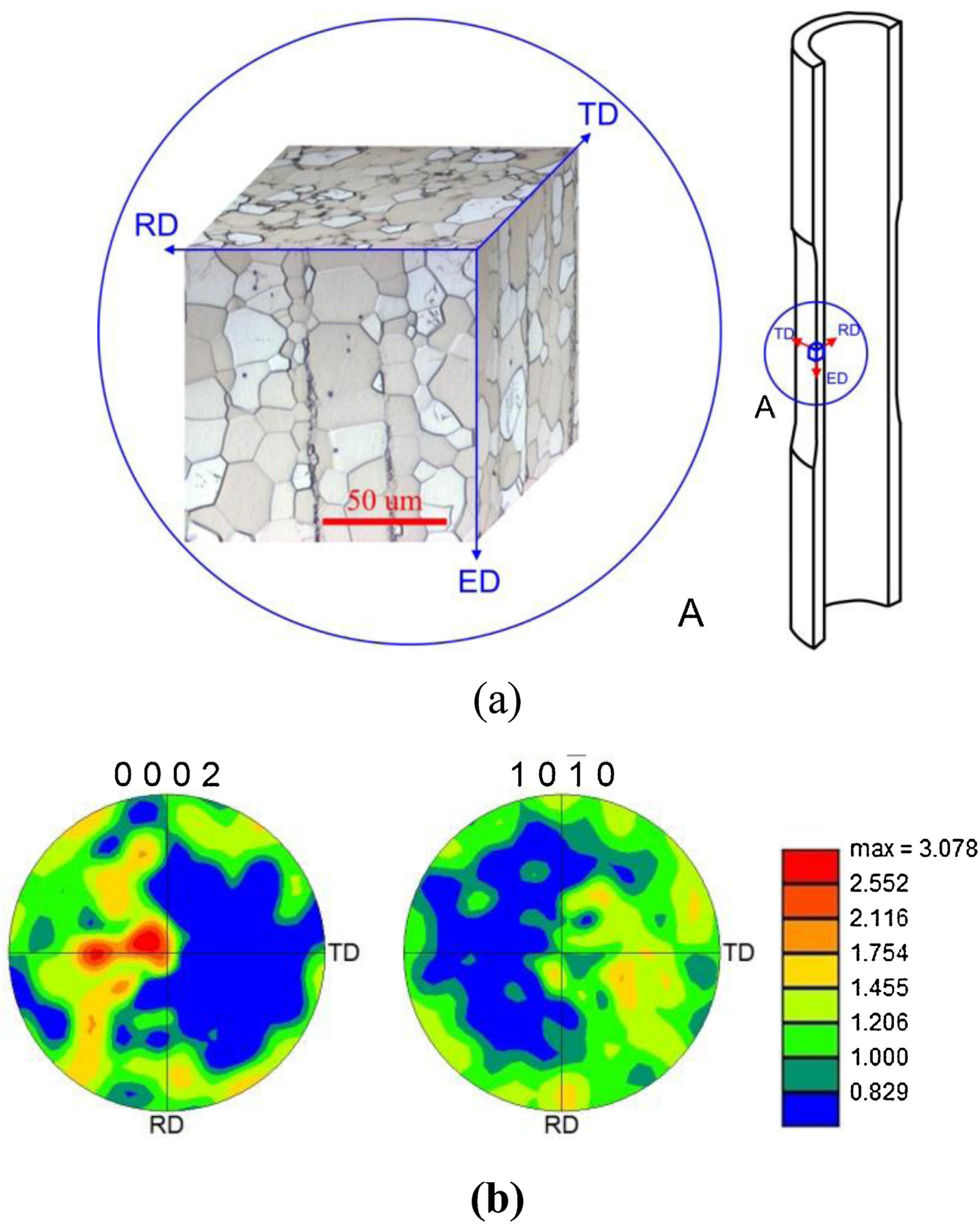

Fig. 1. Initial microstructure and texture of extruded GW83 alloys: (a) three-dimensional microstructure, (b) (0002) and {10-10} pole figures on the RD-TD plane.

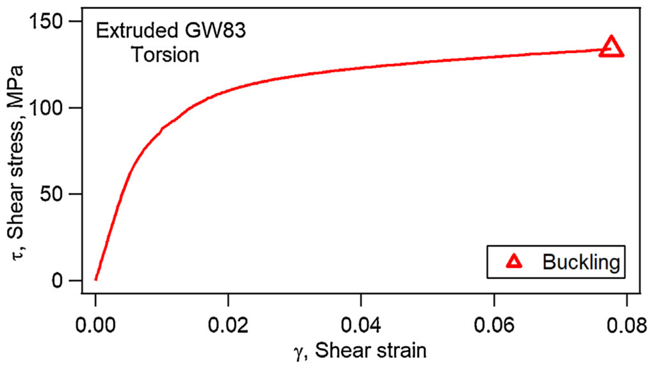

Fig. 2. Shear stress-shear strain curve of extruded GW83 alloy.

2. Experimental

2.1. Material and specimen

An extruded Mg-8.0Gd-3.0Y-0.5 Zr (wt%) bar with a diameter of 36 mm was employed in this study. The bar was extruded at 450 °C with an extrusion ratio of 25:1. Solid specimens for monotonic pure torsion experiments were machined from the extruded bar. The diameter and gage length was 24.0 mm and 30.0 mm, respectively. Pure torsion experiments was examined at room temperature with a rotating rate of 2°/s. The torsion direction was perpendicular to the extrusion direction. More experimental details on specimen preparation and microstructure observation can be founding in the Reference [13].

Fig. 1(a) shows the initial optical microstructure on the ED-RD, ED-TD and RD-TD (RD-radial direction, TD-transverse direction) planes of extruded GW83 alloy. The average size of equiaxial grains in the three planes is about 25 μm. Several extrusion bands can be seen in the matrix and parallel to the extrusion direction. Fig. 1(b) displays (0002) and {10-10} pole figures on the RD-TD plane of extruded GW83 alloy. It can be seen that extruded GW83 alloy displays a weakened texture. The intensity of (0002) pole is much lower than that of the conventional extruded Mg alloys.

2.2. Mechanical experiments

Cyclic torsion experiments were performed by using tubular specimens with their axes along extrusion direction. The outer and inner diameter were 24 mm and 20 mm, respectively. The gage length of the shear extensometer was 25.4 mm. The shear strain amplitudes were controlled in the experiments and they ranged from 0.606% to 4.157%. More experimental details on fatigue test processing and microstructure observation can be founding in the Reference [13]. The tension-compression fatigue properties of extruded GW83 alloy from Reference [13] and shear fatigue properties of extruded AZ31B and AZ61A alloys from Reference [21,23] are used to compare with the fatigue data of extruded GW83 alloy from the current study.

3. Results and discussions

3.1. Mechanical properties under pure torsion

Fig. 2 shows the shear stress-shear strain curve obtained from monotonic pure torsion of extruded GW83 alloy at a rotating rate of 2°/s. From the pure torsion test, the shear modulus is found to be 17.8 GPa. The 0.2% yield strength in shear is approximately 52 MPa. The stress-strain curve of the extruded GW83 alloy obtained from the monotonic tension experiment has been studied in an earlier paper [13]. The yield stress, ultimate tensile stress and elongation are 205 MPa, 307 MPa and 16.4%. Similar to the properties under monotonic tension, extruded GW83 alloy displays work hardening before buckling under torsion.

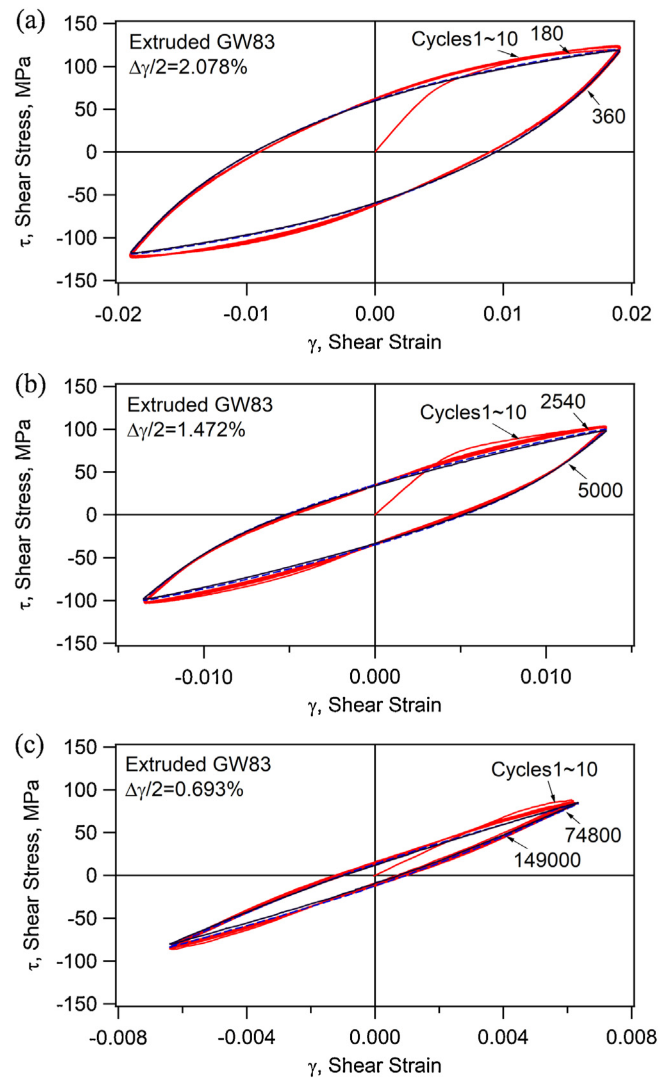

Fig. 3. Shear stress-shear strain hysteresis loops of extruded GW83 alloy: (a) $\Delta\gamma/2 = 2.078\%$; (b) $\Delta\gamma/2 = 1.472\%$; (c) $\Delta\gamma/2 = 0.693\%$.

3.2. Cyclic torsion

Fig. 3 shows the shear stress-shear strain hysteresis loops of extruded GW83 alloy obtained from cyclic torsion at the three strain amplitudes of 2.078%, 1.472% and 0.693%, respectively. The stress-strain hysteresis loops of the first 10 cycles, half-life cycle together with the fatigue-life cycle are plotted in the figure. The extruded GW83 alloy presents a perfectly symmetric shape of shear stress-strain hysteresis loop under cyclic torsion at the three tested strain amplitudes. Fig. 4 shows the variations of the shear stress amplitudes with the number of loading cycles at shear strain amplitudes ranging from 0.606% to 2.425%. When the shear strain amplitude is lower than 1.732%, the extruded GW83 alloy displays slight cyclic softening first and then marginal cyclic hardening. The cyclic hardening behavior is due to the increased dislocation slips and small volume fraction of extension twinning. On the other hand, when the strain amplitude is higher than 1.732%, the material displays cyclic softening until final fracture. The cyclic softening behavior at higher strain amplitudes may be

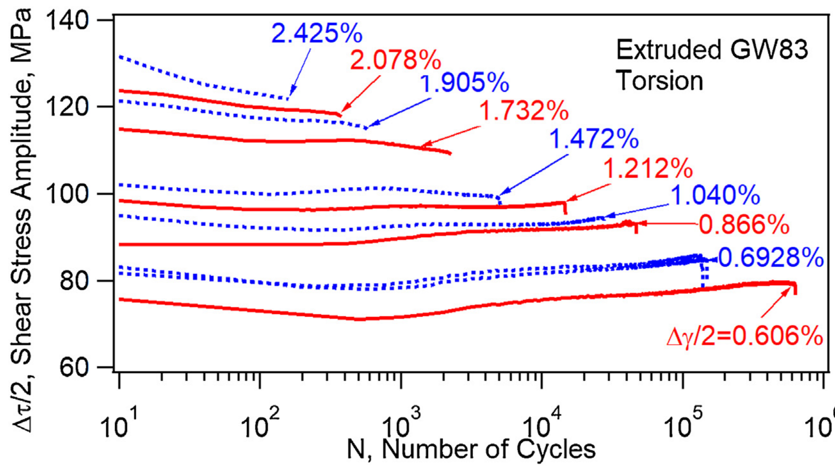

Fig. 4. Variation of shear stress amplitude with number of loading cycles under shear strain amplitudes from 0.606% to 2.425% for extruded GW83 alloy.

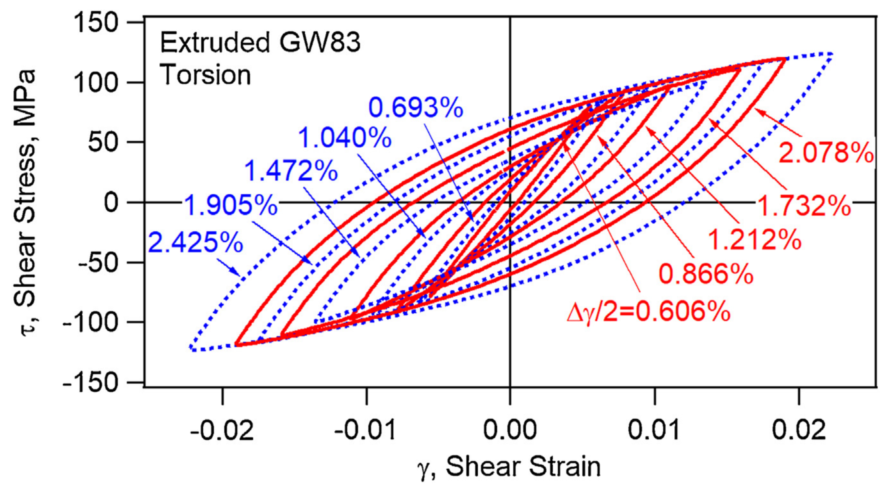

Fig. 5. Stabilized shear stress-shear strain hysteresis loops at half-life cycles.

Table 1
Shear fatigue results for extruded GW83 alloy obtained from free end torsion experiments.

Spec ID	$\Delta\gamma/2$ (%)	$\Delta\varepsilon_{eq}/2$ (%)	$\Delta\tau/2$ (MPa)	τ_m (MPa)	ΔW^p (MJ/m^3)	N_f
83IITU30	4.157	2.4	135.8	0.42	–	39
83IITU35	2.915	1.68	128.3	0.34	–	78
83IITU23	2.425	1.4	123.5	0.42	4.389	175
83IITU36	2.078	1.2	119.2	0.46	3.233	382
83IITU27	1.905	1.1	116.7	0.21	2.714	583
83IITU17	1.732	1.0	110.9	0.17	2.060	2,275
83IITU28	1.472	0.85	99.9	0.12	1.396	5,083
83IITU22	1.212	0.7	97.1	−0.05	0.916	14,700
83IITU20	1.040	0.6	93.2	0.35	0.680	27,780
83IITU21	0.866	0.5	92.3	0.71	0.400	47,000
83IITU18	0.693	0.4	83.9	0.22	0.213	149,653
83IITU31	0.606	0.35	79.2	−1.04	0.105	630,619

$\Delta\gamma/2$ = Shear strain amplitude; $\Delta\varepsilon_{eq}/2$ = Equivalent strain amplitude; $(\Delta\varepsilon_{eq}/2) = {}^{(\Delta\gamma/2)}/\sqrt{3}$; $\Delta\tau/2$ = Stabilized shear stress amplitude; τ_m = Stabilized mean stress; ΔW^p = Plastic strain energy density per loading cycle; N_f = Number of cycles to failure.

attributed to the increased volume fraction of extension twinning.

Fig. 5 shows the stabilized shear stress-shear strain hysteresis loops with the shear strain amplitudes ranging from 0.606% to 2.425%. The enveloped area stands for the strain energy density per loading cycle at each shear strain amplitude. A careful comparison of the upper branch and the lower branch of the stress-strain hysteresis loop reveals complete symmetry of the shape for all the cases shown in Fig.5. As a comparison, the stress-strain hysteresis loops of extruded GW83 alloy is nearly symmetric at a strain amplitude below 1.2% under cyclic tension-compression. The asymmetry in the stress-strain hysteresis loop under tension-compression at a higher strain amplitude is due to twinning-detwinning [13]. For cyclic torsion, the symmetric stress-strain hysteresis loop at all range of strain amplitudes suggests that the mechanism of plastic deformation is identical during loading and during reversed loading.

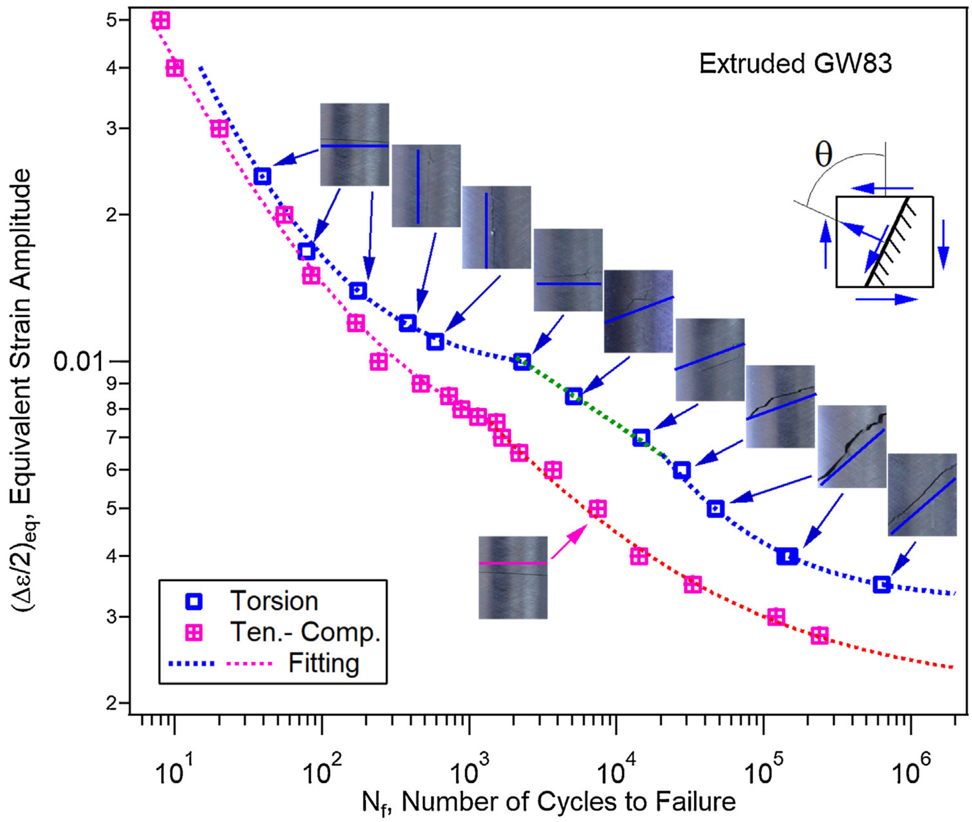

Fig. 6. Strain-life fatigue curves of torsion and tension-compression for extruded GW83 alloy.

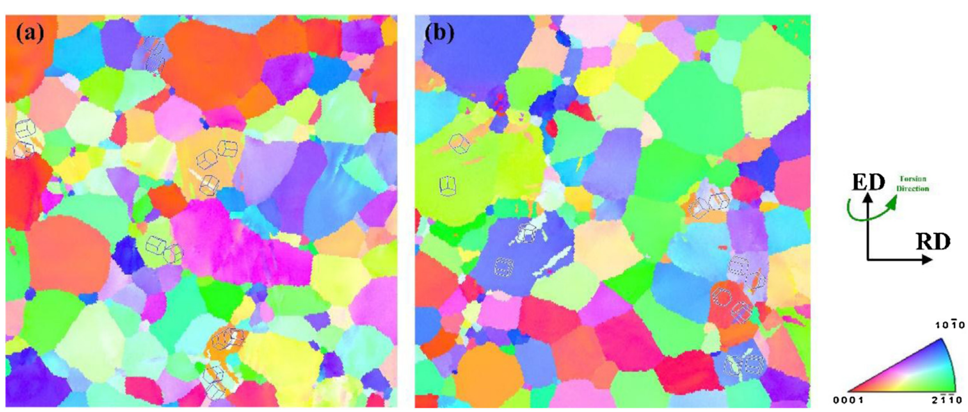

Fig. 7. IPF map of extruded GW83 alloy after cyclic torsion: (a) $\Delta\gamma/2 = 0.693\%$; (b) $\Delta\gamma/2 = 4.157\%$.

3.3. Shear fatigue life

Table 1 summarizes the shear fatigue results of extruded GW83 alloy obtained from cyclic torsion along the extrusion direction. The stress and strain quantities presented in Table 1 are taken from the stabilized stress-strain hysteresis loops at approximately half fatigue lives. The strain values of the two largest amplitudes were not measured directly from the extensometer due to the limit in the range of the extensometer. They were estimated from the rotational angle of the testing machine. As a result, these two specimens did not have plastic strain energy density values. When the stress decreased by 5% from the maximum stress, the fatigue experiment was terminated. For most cases, a fatigue experiment was terminated when a visible fatigue crack appeared on the specimen surface. Due to symmetrical stress-strain hysteresis loops, the mean stresses are virtually zero for the fully reversed strain-controlled cyclic torsion.

Fig. 6 shows the shear strain-life fatigue curve of the extruded GW83 alloy. For a comparison, the tension-compression fatigue results of extruded GW83 alloy from Reference [13] are also presented. The blue markers represent the results of cyclic torsion and the open circles denote the results of cyclic tension-compression. It is clear in Fig. 6 that two kink points exist in the shear strain-life fatigue curve. The kink points for extruded GW83 alloy correspond to shear strain amplitudes of 1.040% and 1.732%, and the fatigue life of 27,800 and 2300 cycles, respectively. The strain-life fatigue curves can be described by the following equation:

$$\left(\frac{\Delta\varepsilon_{eq}}{2} - \varepsilon_0\right)^{\xi} N_f = C \quad (1)$$

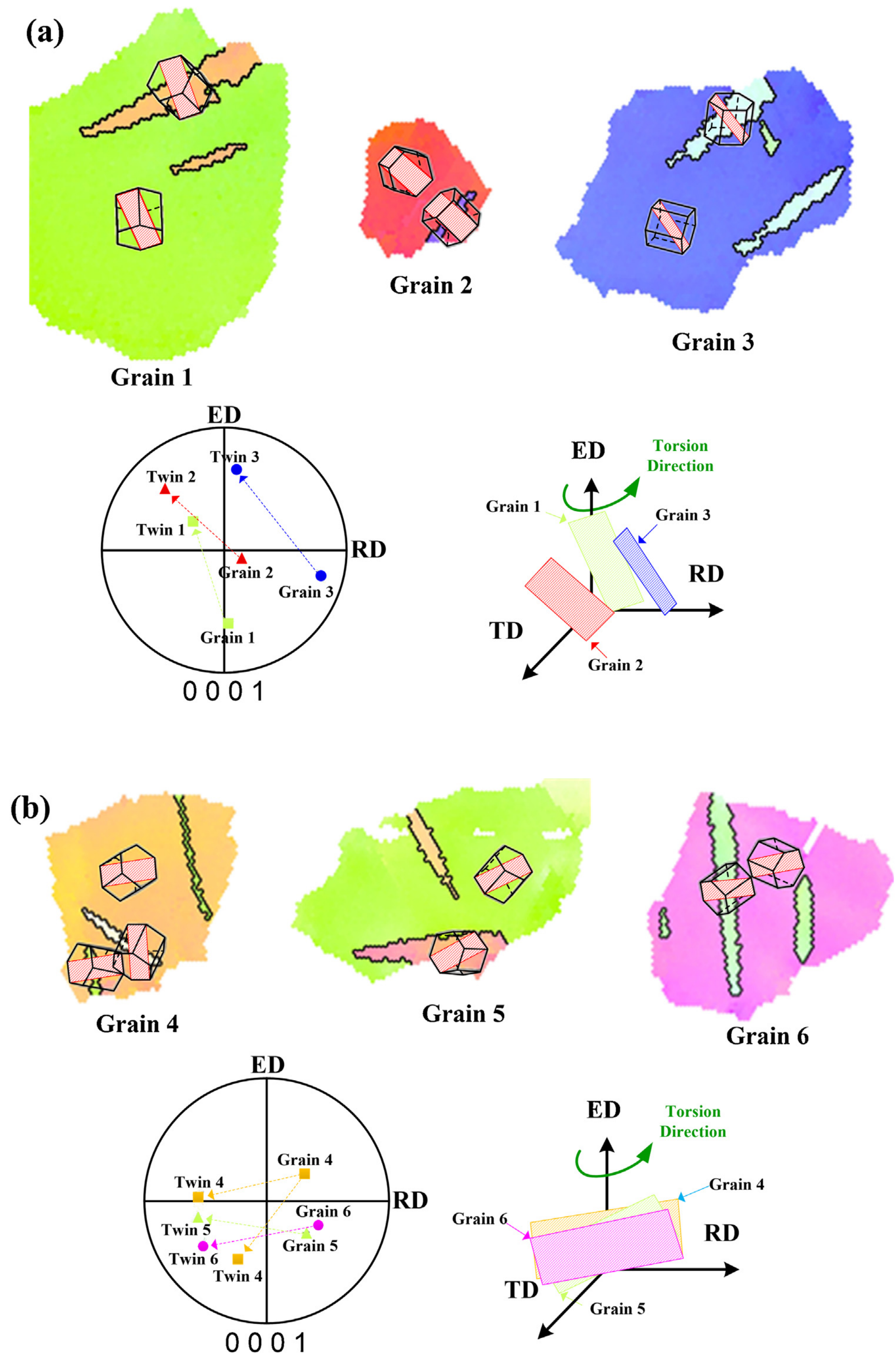

Fig. 8. Extension {10–12} twins in extruded GW83 alloy after cyclic torsion at shear strain amplitudes of (a) $\Delta\gamma/2 = 0.693\%$; (b) $\Delta\gamma/2 = 4.157\%$. The grain orientations and shear planes corresponding to the parent grains and extension twins were added in the figure.

where $\Delta\varepsilon_{eq}/2$ is strain amplitude, N_f is number of cycles to failure, and ε_0, ξ and C are fitting parameters. The shear fatigue curve can be divided by two kink points into three parts and each part can be described by Eq. (1). For a shear strain amplitude lower than 1.04%, the constants in Eq. (1) are ε_0 =0.0032, ξ =1.38 and C =0.0032. For a shear strain amplitude larger than 1.732%, the constants in Eq. (1) are ε_0 =0.0094, ξ =1.31 and C =0.157. For a strain amplitude ranging from 1.040% to 1.732%, the constants in Eq. (1) are 6.0×10^{-6}, ξ =4.94 and $C = 3.0 \times 10^{-7}$.

The early fatigue crack macrographs corresponding to strain amplitudes are inserted in the strain-life fatigue curves. The vertical and horizontal directions are extruded and radial directions, respectively. The fatigue cracks under tension-compression are initiated on the maximum tensile planes at all tested strain amplitudes [13]. Under pure torsion, the fatigue cracks are initiated on the maximum shear planes when the shear strain amplitude is higher than the upper kink point. When the shear strain is lower than the lower kink point, early fatigue crack is consistently initiated on the

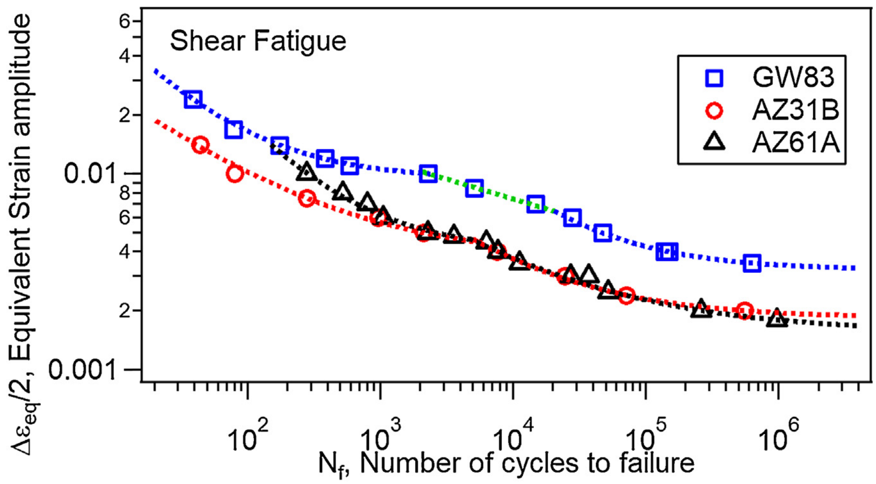

Fig. 9. Strain-life fatigue curve of shear fatigue for extruded GW83, AZ31B [23] and AZ61A [21,24] alloys.

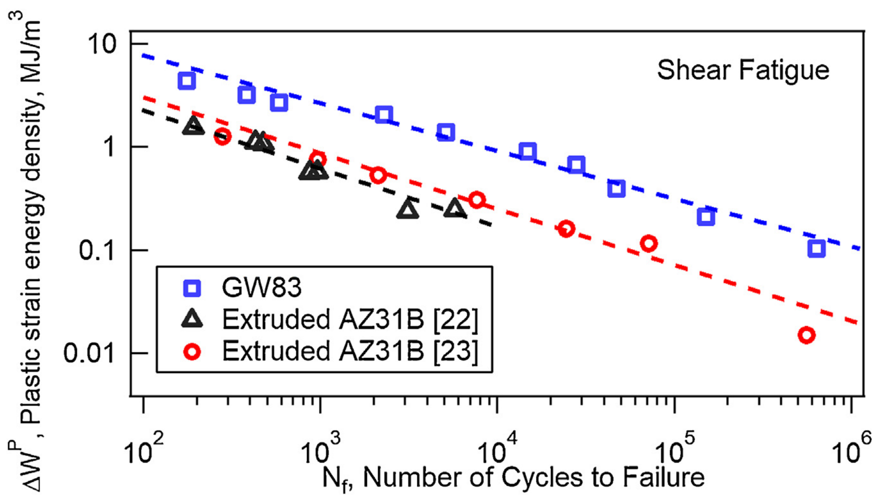

Fig. 10. Relationship between plastic strain energy density and fatigue lives [22,23].

maximum tensile planes (±45° from extrusion direction). When the shear strain is in between the two kink points, early fatigue crack is approximately ±22.5° from the extrusion direction. The cracking behavior is dependent on the strain amplitude under pure shear loading. The cracking results are similar to these found in fatigue of 7075-T651 aluminum alloy under pure shear [25].

4. Further discussions

4.1. Microstructure

Fig. 7 shows the inverse pole figure map on ED-RD plane after fatigue at shear strain amplitudes of 0.693% and 4.157%, respectively. Few residual twins are observed at the two shear strain amplitudes. As seen from the grain orientation, the c-axis of the twins is tilted about 86.3°with respect to the c-axis of parent grains. It demonstrates that the residual twins are extension twins in the shear fatigue. In addition, the volume fraction of twins at the shear strain amplitude of 0.693% is less than that of shear strain amplitude of 4.157%.

Fig. 8 shows the detailed information of the residual twins at shear strain amplitudes of 0.693% and 4.157%. The grain orientations and shear planes corresponding to the parent grains and extension twins are added in the figure. At a shear strain amplitude of 0.693%, residual twins are observed for grains of different orientations with yellow denoting grain 1, blue for grain 2 and red for grain 3, as shown in the Fig. 8(a). The c-axes of Grain 1, Grain 2 and Grain 3 are approximately parallel to the extrusion direction, transverse direction and radial direction, respectively. The twinning plane of {10–12} extension twins of the three grains are titled approximately 45° from the RD-TD plane. The fatigue fracture plane is parallel to the maximum tensile plane at the low shear strain amplitudes, resulting in tensile cracking. Moreover, there are two extension twins with identical variants in Grain 1 and Grain 2. No twin-twin interaction or twin pair is detected at the low shear strain amplitude.

At a shear strain amplitude of 4.157%, there are several residual twins observed in Grain 4, Grain 5 and Grain 6, as shown in Fig. 8(b). The c-axes of the grains are tilted from the radial and transverse directions. It is noticed that the twinning plane of {10–12} extension twins of the three grains are approximately parallel to the extrusion direction. The fatigue fracture plane is parallel or perpendicular to the RD-TD plane at high shear strain amplitudes, resulting in the observed shear cracking. Furthermore, there are two extension twins with identical variants in the Grain 5 and Grain 6. Two different extension twin variants are observed in the Grain 4. No compression twins nor secondary twins are detected at the high shear strain amplitude.

Earlier study indicates that the strain-life fatigue curves of extruded GW83 alloy under tension-compression fatigue display a distinct kink point. When the strain amplitude is higher than 0.75%, the material presents near symmetric stress-strain hysteresis loop and twinning-detwinning plays a dominant role in the plastic deformation [13]. For all the shear strain amplitudes under cyclic torsion, twinning and detwinning take place during cyclic torsion deformation. The volume fraction of residual twins under cyclic torsion is much less than that of cyclic tension-compression deformation.

4.2. Shear fatigue life of extruded alloys

Fig. 9 shows the shear fatigue lives of the strong and weak texture Mg alloys. The extruded GW83 alloy has weak basal texture and shows two kink points in the shear fatigue life. The extruded AZ31B and AZ61A alloys have strong basal texture and shows a kink point in the shear fatigue life [21,23,24]. The extruded GW83 alloy presents much higher shear fatigue lives than those of extruded AZ31B and AZ61A alloys loading along the extrusion direction at an identical shear strain amplitude. Moreover, the shear fatigue lives of extruded AZ31B alloy are almost identical with those of extruded AZ61A alloy at low stain amplitudes.

Fig. 10 displays the relationship between the plastic strain energy density per loading cycle and fatigue lives of extruded GW83 and AZ31B alloys. Results of extruded AZ31B alloy were taken from References [22,23]. The plastic strain energy density per loading cycle as a fatigue parameter correlate fatigue experiments under tension-compression and under pure shear well for extruded AZ31B alloy. At the same plastic strain energy density, the fatigue life of extruded GW83 alloy is much higher than that of extruded AZ31B alloy.

5. Conclusions

Deformation and fatigue of extruded GW83 alloy were experimentally investigated by carrying out torsion experiments using tubular specimens along the extrusion direction. The main conclusions can be drawn as follows:

(1) Twinning and detwinning of extension twins take place during cyclic torsion. The shear stress-shear strain hysteresis loops display a perfectly symmetric shape at all tested strain amplitudes. Marginal cyclic softening is observed when the shear strain amplitude is higher than 1.732%.
(2) The strain-life fatigue curve shows two kink points, corresponding to the shear strain amplitude of 1.040% and 1.732%, respectively. The kink points signify different cracking behavior under pure shear loading.
(3) At an identical strain amplitude, the fatigue life under pure shear is much higher than that under tension-compression.

Acknowledgements

Fenghua Wang, Jie Dong and Zhenyan Zhang gratefully acknowledge the support of the National Natural Science Foundation of China (51601112), Shanghai Rising-Star Program (17QB1403000, 16QB1402800). Miaolin Feng thanks support by National Natural Science Foundation of China (11572191). Yanyao Jiang thanks support from the National Science Foundation (CMMI-1762312).

References

[1] X.J. Wang, D.K. Xu, R.Z. Wu, X.B. Chen, Q.M. Peng, L. Jin, Y.C. Xin, Z.Q. Zhang, Y. Liu, X.H. Chen, G. Chen, K.K. Deng, H.Y. Wang, J. Mater. Sci. Technol. 34 (2018) 245–247.
[2] B.J. Wang, S.D. Wang, D.K. Xu, E.H. Han, J. Mater. Sci. Technol. 33 (2017) 1075–1086.
[3] Y.N. Wang, J.C. Huang, Acta Mater. 55 (2007) 897–905.
[4] A.S. Khan, A. Pandey, T. Gnäupel-Herold, R.K. Mishra, Int. J. Plast. 27 (2011) 688–706.
[5] X.Y. Lou, M. Li, R.K. Boger, S.R. Agnew, R.H. Wagoner, Int. J. Plast. 23 (2007) 44–86.
[6] F. Pan, M. Yang, X. Chen, J. Mater. Sci. Technol. 32 (2016) 1211–1221.
[7] H. Pan, F. Wang, L. Jin, M. Feng, J. Dong, J. Mater. Sci. Technol. Res. 32 (2016) 1282–1288.
[8] Q. Li, Q. Yu, J. Zhang, Y. Jiang, Scripta Mater. 64 (2011) 233–236.
[9] L. Wu, A. Jain, D.W. Brown, G.M. Stoica, S.R. Agnew, B. Clausen, D.E. Fielden, P.K. Liaw, Acta Mater. 56 (2008) 688–695.
[10] S. Dong, Q. Yu, Y. Jiang, J. Dong, F. Wang, L. Jin, W. Ding, Int. J. Plast. 91 (2017) 25–47.
[11] S.M. He, X.Q. Zeng, L.M. Peng, X. Gao, J.F. Nie, W.J. Ding, J. Alloys Compd. 421 (2006) 309–313.
[12] S.M. He, X.Q. Zeng, L.M. Peng, X. Gao, J.F. Nie, W.J. Ding, J. Alloys Compd. 427 (2007) 316–323.
[13] F. Wang, J. Dong, Y. Jiang, W. Ding, Mater. Sci. Eng. A 561 (2013) 403–410.
[14] S. Dong, F. Wang, Q. Wan, J. Dong, W. Ding, Y. Jiang, Mater. Sci. Eng. A 641 (2015) 1–9.
[15] S. Biswas, B. Beausir, L.S. Toth, S. Suwas, Acta Mater. 61 (2013) 5263–5277.
[16] J. Yu, Z. Zhang, P. Xu, B. Dong, Q. Wang, M. Meng, H. Hao, X. Li, X. Yin, J. Alloys Compd. 787 (2019) 239–253.
[17] X.Q. Guo, W. Wu, P.D. Wu, H. Qiao, K. An, P.K. Liaw, Scripta Mater. 69 (2013) 319–322.
[18] B. Song, H. Pan, L. Chai, N. Guo, H. Zhao, R. Xin, Mater. Sci. Eng. A 689 (2017) 78–88.
[19] J. Hu, H. Gao, Y. Meng, Z. Zhang, L. Gao, Mater. Sci. Eng. A 726 (2018) 215–222.
[20] N. Guo, B. Song, C. Guo, R. Xin, Q. Liu, Mater. Des. 83 (2015) 270–275.
[21] J. Zhang, Q. Yu, Y. Jiang, Q. Li, Int. J. Plast. 27 (2011) 768–787.
[22] J. Albinmousa, H. Jahed, S. Lambert, Int. J. Fatigue 33 (2011) 1403–1416.
[23] Y. Xiong, Q. Yu, Y. Jiang, Mater. Sci. Eng. A 546 (2012) 119–128.
[24] Q. Yu, J. Zhang, Y. Jiang, Q. Li, Int. J. Fatigue 33 (2011) 437–447.
[25] T. Zhao, Y. Jiang, Int. J. Fatigue 30 (2008) 834–849.